

PAPER • OPEN ACCESS

Mathematical modeling of elastic soil acid treatment

To cite this article: O V Galtsev 2021 *J. Phys.: Conf. Ser.* **1902** 012108

View the [article online](#) for updates and enhancements.

You may also like

- [On homogenized equations of filtration in two domains with common boundary](#)
A. M. Meirmanov, O. V. Galtsev and S. A. Gritsenko
- [Numerical implementation of the Lamé equation with complex boundary conditions](#)
S B Sorokin, A G Maksimova, G G Lazareva et al.
- [The Nahm equations, finite-gap potentials and Lamé functions](#)
R S Ward



ECS The Electrochemical Society
Advancing solid state & electrochemical science & technology

242nd ECS Meeting

Oct 9 – 13, 2022 • Atlanta, GA, US

Early hotel & registration pricing ends September 12

Presenting more than 2,400 technical abstracts in 50 symposia

The meeting for industry & researchers in

BATTERIES
ENERGY TECHNOLOGY
SENSORS AND MORE!

 Register now!

 **ECS Plenary Lecture featuring M. Stanley Whittingham,**
Binghamton University
Nobel Laureate –
2019 Nobel Prize in Chemistry



Mathematical modeling of elastic soil acid treatment

O V Galtsev

Department of Information and Robotic Systems, Belgorod State National Research University, 85 Pobedy St., Belgorod, 308015, Russia

E-mail: galtsev_o@bsu.edu.ru

Abstract. The study is devoted to an initial boundary value problem describing the process of cleaning the bottomhole zone of an oil well with acid solution. It is assumed that the soil frame is an elastic solid body and the pore space has double porosity. The physical process is described at the microscopic level by the Stokes equations for the liquid component, the diffusion-convection equation for the concentrations of acid and chemical reaction products, and the Lamé equations for the solid frame. Due to soil dissolution, the pore space has an unknown (free) boundary. The lattice Boltzmann method (LBM), the immersed boundary method (IBM) and the finite element method (FEM) are used for computer simulation. Finally, discretization of equations and results of numerical solutions are presented.

1. Introduction

The bottomhole cleaning process (see figure 1) is very important to increase oil production. Oil reservoirs are complex geologically heterogeneous objects. Heterogeneity means that the medium properties change in space. The analysis of wells and cores shows that the geological properties (porosity, permeability, etc.) of oil reservoirs are heterogeneous even within one field. Often, insufficient consideration of heterogeneity at the planning stage becomes evident too late, when the acid solution pumped into the soil through injection wells is far from the intended place. In addition, the concentration of injected acid and injection modes play an important role. Therefore, understanding the dynamics of fluids in heterogeneous porous media and the mechanism of rock dissolution by acids is of fundamental importance for the effective management of oil production. This can be achieved by creating a hydrodynamic simulator of the bottomhole zone based on the corresponding mathematical model, which allows to optimize the considered technological process.

There is a wide range of mathematical models describing the process of rock dissolution at the macroscopic level (see [1–3], and references therein), where typical dimensions are meters or tens of meters. At the macroscopic level, at each point of the continuous medium, there is both a solid frame (rock) and a liquid in the pores of this frame. All such models are based on the same principle. Fluid dynamics are usually described by the Darcy system of filtration equations or some of its modification. Equations describing the migration of acid and chemical reaction products are simply postulated and are modified diffusion-convection equations for the corresponding concentrations. The main thing in these postulates is the form of coefficients in equations, because the main mechanism of the physical process is concentrated on the free boundary between the pore space and the solid frame. Moreover, during the process, the geometry of the pore space changes. All these fundamentally important changes occur at



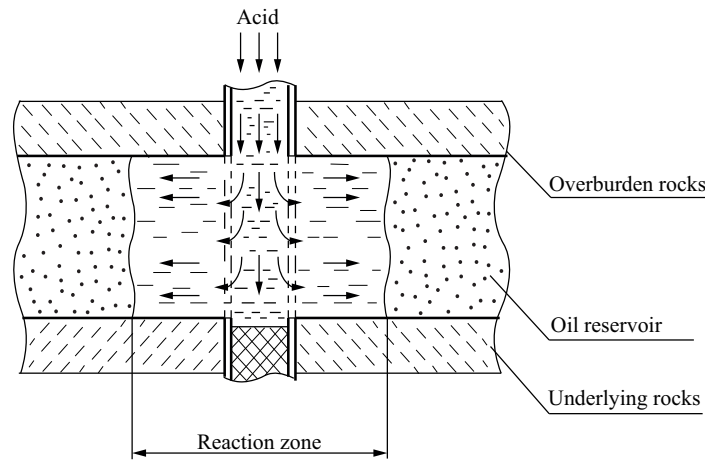


Figure 1. Bottom hole cleaning process.

the microscopic level, corresponding to the average size of pores or cracks in rocks, while any of the proposed macroscopic models operates on completely different scales.

The exact formulation of rock dissolution problem in one porosity medium for an absolutely rigid solid body at the microscopic level was first presented in the monograph [4], but mathematically rigorous results on the existence of any solution were absent there.

This paper deals with a more complex problem, where pores of size $\varepsilon = l/L$ and cracks of size $\delta = \varepsilon^\nu$ ($0 < \nu < 1$) are taken into account in elastic soil. Here l is the characteristic pore size and L is the characteristic size of the considered physical region.

Pores are modeled by the system of cylindrical channels of radius $\varepsilon r_p(\mathbf{x}, t)$, $0 < r_p < 1/2$, where its axes are parallel to the axes coordinates located at a distance ε from each other. Cracks are modeled by sphere of radius $\delta r_c(\mathbf{x}, t)$, $0 < r_c < 1/2$, located at a distance δ from each other. The motion of viscous fluid in an elastic periodic skeleton with double porosity was previously considered by A.M. Meirmanov [5].

Here the physical process at the microscopic level is described by the laws of continuum mechanics. These are the Stokes equations for the velocity \mathbf{v}^ε and the pressure p^ε of a viscous incompressible fluid in domain $\Omega_f^\varepsilon(t)$ with dimensionless viscosity κ_μ , Lamé equations for displacement \mathbf{w}^ε of elastic solid frame $\Omega_s^\varepsilon(t)$, diffusion-convection equation for the acid concentration c^ε and the conditions on a strong discontinuity (the required free boundary) $\Gamma^\varepsilon(t)$ “elastic frame-pore space” [6]. There are no inertial terms in the Stokes and Lamé equations, as it has a sufficiently long duration in time (the fluid filtration rate is several meters per year)

The problem is supplemented by the boundary conditions on the free boundary separating the pore space and the soil frame, which follow from the conservation laws of classical mechanics in its integral form, boundary conditions at given boundaries, initial conditions, and an additional condition on the free boundary

$$d_n^\varepsilon = \kappa c^\varepsilon, \quad \kappa = \text{const} > 0, \quad (1)$$

following from the laws of theoretical chemistry [7] and allowing to define this boundary. Here d_n^ε is the velocity $\Gamma^\varepsilon(t)$ in the direction of unit normal \mathbf{n} to the boundary $\Gamma^\varepsilon(t)$, c^ε is the concentration of acid in the liquid, κ is a given constant.

2. Materials and methods

The physical process is considered in a bounded domain Ω (see figure 2) with piecewise Lipschitz boundary S , $\bar{S} = \partial\Omega$, $S = S^0 \cup S^1 \cup S^2$, $S^i \cap S^0 = \emptyset$, $i = 1, 2$, $S^1 \cap S^2 = \emptyset$, $\Omega_T = \Omega \times (0, T)$.

The domain $\Omega_f^\varepsilon(t) \subset \Omega$ describes the region occupied by liquid, and $\Omega_s^\varepsilon(t) \subset \Omega$ denotes elastic frame (see figure 2). The boundary S^0 is impermeable to fluid in the pore space, the boundary S^1 models the injection well.

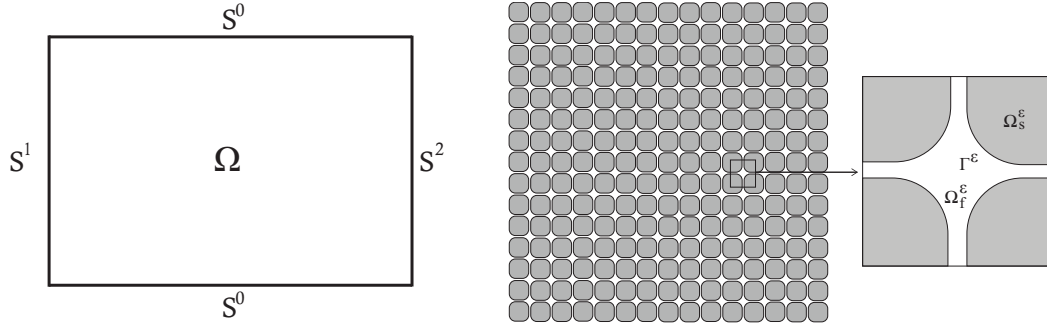


Figure 2. Domain under consideration and periodic pore space.

In dimensionless variables

$$\mathbf{x} = \frac{\mathbf{x}'}{L}, \quad t = \frac{t'}{\tau}, \quad \mathbf{v} = \frac{\tau \mathbf{v}'}{L}, \quad p = \frac{\bar{p}}{p_a},$$

the dynamics of acid solution in an unknown domain $\Omega_f^\varepsilon(t)$ (fluid domain) is described by the system of differential equations

$$\nabla \cdot \mathbb{T}_f^\varepsilon = 0, \quad \nabla \cdot \mathbf{v}^\varepsilon = 0, \quad (2)$$

$$\mathbb{T}_f^\varepsilon = \kappa_\mu \sigma(x, \mathbf{v}^\varepsilon) - p^\varepsilon \mathbb{I},$$

$$\frac{\partial c^\varepsilon}{\partial t} = \nabla \cdot (\kappa_c \nabla c^\varepsilon - \mathbf{v}^\varepsilon c^\varepsilon), \quad (3)$$

$$\frac{\partial c_i^\varepsilon}{\partial t} + \mathbf{v}^\varepsilon \cdot \nabla c_i^\varepsilon = \nabla \cdot (\kappa_i \nabla c_i^\varepsilon), \quad i = 1, \dots, n, \quad (4)$$

for the velocity \mathbf{v}^ε and the pressure p^ε of continuous medium, p_a is atmospheric pressure, c^ε is the reagent concentration, \mathbb{I} is a unit matrix.

In elastic frame $\Omega_s^\varepsilon(t)$ the displacements of continuous medium \mathbf{w}^ε are described by the Lamé equations

$$\nabla \cdot \mathbb{T}_s^\varepsilon = 0, \quad \nabla \cdot \mathbf{w}^\varepsilon = 0. \quad (5)$$

$$\mathbb{T}_s^\varepsilon = \kappa_\lambda \mathbb{D}(x, \mathbf{w}^\varepsilon) - p^\varepsilon \mathbb{I}.$$

Let $\Gamma^\varepsilon(t) = \partial\Omega_f^\varepsilon(t) \cap \partial\Omega_s^\varepsilon(t)$ be a free boundary, $\mathbf{x}_0 \in \Gamma^\varepsilon(t)$ and $\mathbf{n}(\mathbf{x}_0, t)$ is the unit normal vector to the boundary $\Gamma^\varepsilon(t)$ at the point \mathbf{x}_0 .

There are boundary condition (1) and conditions on the free boundary $\Gamma^\varepsilon(t)$

$$\begin{aligned} \mathbf{v}^\varepsilon(\mathbf{x}_0 + 0, t) &= \mathbf{v}^\varepsilon(\mathbf{x}_0 - 0, t), & \mathbf{w}^\varepsilon(\mathbf{x}_0 + 0, t) &= \mathbf{w}^\varepsilon(\mathbf{x}_0 - 0, t), \\ v_n^\varepsilon(\mathbf{x}_0 \pm 0, t) &= \mathbf{v}^\varepsilon(\mathbf{x}_0 \pm 0, t) \cdot \mathbf{n}(\mathbf{x}_0, t) = d_n(\mathbf{x}_0, t), \end{aligned} \quad (6)$$

$$\mathbb{T}_f^\varepsilon \cdot \mathbf{n} = \mathbb{T}_s^\varepsilon \cdot \mathbf{n}, \quad (7)$$

$$(d_n^\varepsilon - v_n^\varepsilon) c^\varepsilon + \kappa_c \frac{\partial c^\varepsilon}{\partial n} = -\beta c^\varepsilon, \quad (8)$$

$$(d_n^\varepsilon - v_n^\varepsilon) c_i^\varepsilon + \kappa_i \frac{\partial c_i^\varepsilon}{\partial n} = \beta \beta_i c^\varepsilon, \quad i = 1, \dots, m, \quad (9)$$

$$\frac{\partial c^\varepsilon}{\partial n} = \nabla c^\varepsilon \cdot \mathbf{n},$$

expressing the laws of conservation of mass [8].

In (2)–(9) $v_n^\varepsilon = \mathbf{v} \cdot \mathbf{n}$ is the normal component of the fluid velocity vector \mathbf{v} , \mathbf{n} is the unit normal vector to the free boundary $\Gamma^\varepsilon(t)$, outer with respect to the region $\Omega_f^\varepsilon(t)$, κ_c , κ_i , β and β_i ($i = 1, \dots, m$) are given positive constants, \mathbf{v}^ε and p^ε are the velocity and pressure in the liquid, c_i^ε are concentrations of chemical reactions products.

Condition (6) simplifies the boundary condition (8)

$$\kappa_c \frac{\partial c^\varepsilon}{\partial n} = -\beta c^\varepsilon. \quad (10)$$

On the given boundaries, consisting of the injection well S^1 , the lateral boundary S^2 and the impermeable boundary S^0 , the following conditions are satisfied

$$\mathbf{v}^\varepsilon = 0, \quad \mathbf{x} \in S^0, \quad t > 0, \quad (11)$$

$$\mathbb{T}^\varepsilon \cdot \mathbf{n} = -p^i \mathbf{n}, \quad i = 1, 2, \quad \mathbf{x} \in S^1, \quad t > 0, \quad (12)$$

$$\frac{\partial c^\varepsilon}{\partial n} = 0, \quad \mathbf{x} \in S^0, \quad t > 0, \quad (13)$$

$$c^\varepsilon = c^1 = \text{const} \geq 0, \quad \mathbf{x} \in S^1, \quad t > 0, \quad (14)$$

$$\nabla c_i^\varepsilon \cdot \mathbf{n} = 0, \quad i = 1, \dots, k, \quad \mathbf{x} \in S^1, \quad t > 0, \quad (15)$$

$$c_i^\varepsilon = 0, \quad i = 1, \dots, m, \quad \mathbf{x} \in S^0, \quad t > 0. \quad (16)$$

In (8)–(16) \mathbf{n} is the unit normal vector to the boundaries S^0 , S^1 , $v_n = \mathbf{v}^\varepsilon \cdot \mathbf{n}$.

The problem is completed by initial conditions

$$c^\varepsilon(\mathbf{x}, 0) = c_0(\mathbf{x}), \quad c_i^\varepsilon(\mathbf{x}, 0) = 0, \quad i = 1, \dots, m, \quad (17)$$

$$r(\mathbf{x}, 0) = r_0(\mathbf{x}), \quad r_p(\mathbf{x}, 0) = r_{p,0}(\mathbf{x}), \quad r_c(\mathbf{x}, 0) = r_{c,0}(\mathbf{x}), \quad (18)$$

$$p_0(\mathbf{x}) = p^0, \quad \mathbf{x} \in S^0, \quad t > 0, \quad (19)$$

$$p_0(\mathbf{x}) = p^1, \quad \mathbf{x} \in S^1, \quad t > 0, \quad p^0 \in \mathbb{C}^2(\bar{\Omega}). \quad (20)$$

For simplicity, assume p^0 , p^1 and c^1 are given positive constants.

Note that the problem (1), (6)–(8), (10)–(14), (17) is solved independently of defining functions c_i ($i = 1, 2, \dots, m$). The latter are determined after finding the functions $\{\mathbf{v}^\varepsilon, p^\varepsilon, c^\varepsilon, r\}$.

All functions of the form $\Phi(\mathbf{x}, t, \mathbf{y}, \mathbf{z})$ are considered 1-periodic in variables \mathbf{y} and \mathbf{z} respectively, where $(\mathbf{x}, t) \in \Omega$ and

$$\mathbf{y}, \mathbf{z} \in Y = \left(-\frac{1}{2}, \frac{1}{2}\right)^3 \subset \mathbb{R}^3, \quad \mathbf{y} = (y_1, y_2, y_3), \quad \mathbf{z} = (z_1, z_2, z_3), \quad |y_i|, |z_i| < \frac{1}{2}.$$

The structure of the pore space $Y_f(r_p)$ is given by the desired function $r_p(\mathbf{x}, t)$, $0 < r_p(\mathbf{x}, t) < 1/2$ as $Y = Y_f \cup \gamma_p \cup Y_s$, $Y_f(r_p) = Y_{f,1}(r_p) \cup Y_{f,2}(r_p) \cup Y_{f,3}(r_p)$, $Y_{f,1}(r_p) = \{\mathbf{y} \in Y : y_2^2 + y_3^2 < r_p^2\}$, $Y_{f,2}(r_p) = \{\mathbf{y} \in Y : y_1^2 + y_3^2 < r_p^2\}$, $Y_{f,3}(r_p) = \{\mathbf{y} \in Y : y_2^2 + y_1^2 < r_p^2\}$ (see figure 3a).

The structure of the crack space is given by the required function $r_c(\mathbf{x}, t)$, $0 < r_c(\mathbf{x}, t) < 1/2$ as $Z_f(r_c) = \{\mathbf{z} \in Z : z_1^2 + z_2^2 + z_3^2 < r_c^2\}$, $Z = Z_f(r_c) \cup \gamma_c \cup Z_s(r_c)$ (see figure 3b).

With a fixed $\varepsilon > 0$ domain $\Omega_f^\varepsilon(t)$ filled with fluid and elastic frame $\Omega_s^\varepsilon(t)$ are determined by the characteristic function $\phi(\mathbf{x}, t, \mathbf{y}, \mathbf{z})$ as follows

$$\Omega_f^\varepsilon(t) = \text{Int}\{\mathbf{x} \in \Omega : \phi^\varepsilon(\mathbf{x}, t) = 1\} = \Omega_{f,p}^\varepsilon(t) \cup \Omega_{f,c}^\varepsilon(t),$$

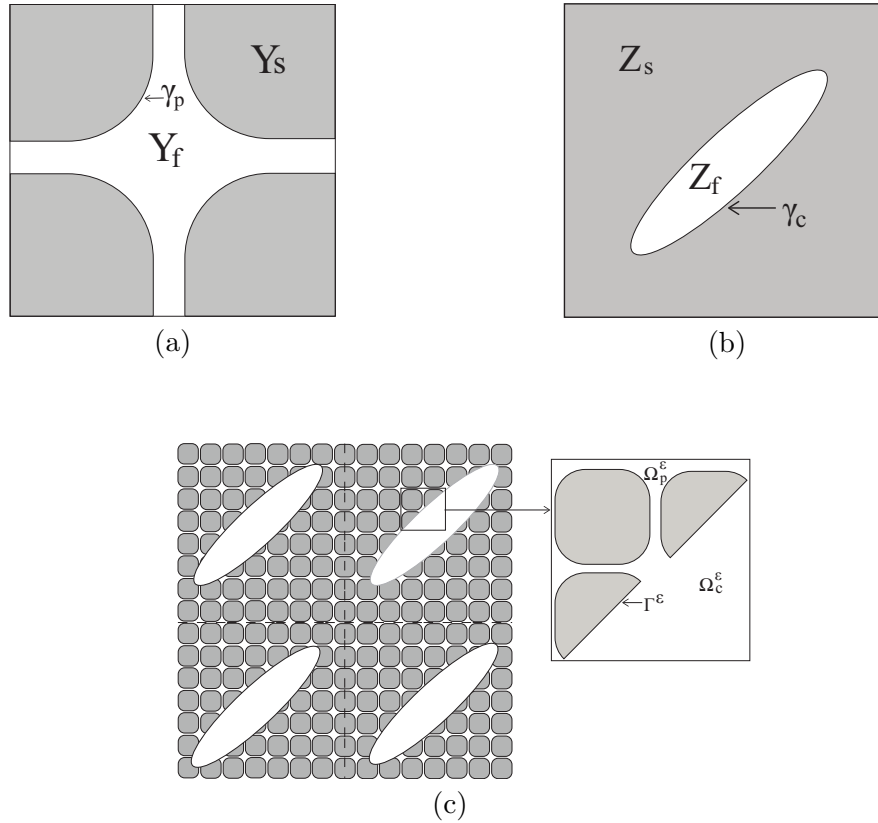


Figure 3. a) unit cell of pore space; b) unit cell of crack; c) cracks and pores.

$$\begin{aligned} \Omega_s^\varepsilon(t) &= \text{Int}\{\mathbf{x} \in \Omega : \phi^\varepsilon(\mathbf{x}, t) = 0\}, \Omega_f^\varepsilon(t) = \text{Int}\{\mathbf{x} \in \Omega : \phi^\varepsilon(\mathbf{x}, t) = 0\}, \\ \phi^\varepsilon(\mathbf{x}, t) &= 1 - (1 - \phi_p^\varepsilon(\mathbf{x}, t))(1 - \phi_c^\varepsilon(\mathbf{x}, t)); \\ \phi_p^\varepsilon(\mathbf{x}, t) &= 1, \mathbf{x} \in \Omega_{f,p}^\varepsilon(t), t > 0, \quad \phi_p^\varepsilon(\mathbf{x}, t) = 0, \mathbf{x} \in \Omega \setminus \overline{\Omega_{f,p}^\varepsilon(t)}, t > 0; \\ \phi_c^\varepsilon(\mathbf{x}, t) &= 1, \mathbf{x} \in \Omega_{f,c}^\varepsilon(t), t > 0, \quad \phi_c^\varepsilon(\mathbf{x}, t) = 0, \mathbf{x} \in \Omega \setminus \overline{\Omega_{f,c}^\varepsilon(t)}, t > 0. \end{aligned}$$

By $d_n^\varepsilon(\mathbf{x}, t)$ we denote velocity of the free boundary in the direction of the normal $\mathbf{n}(\mathbf{x}, t)$ to the surface $\Gamma^\varepsilon(t)$ at the point $\mathbf{x} \in \Gamma^\varepsilon(t)$.

3. Results and discussions

In this study, the lattice Boltzmann method (LBM) was used to solve the system of equations (1)–(4). The method describes the behavior of particles collection and is based on the Boltzmann equation, which describes the gas dynamics on the mesoscopic scale [9]

$$\frac{\partial f}{\partial t} + \mathbf{c} \cdot \nabla_x f = \Theta(f), \quad (21)$$

where f is the particle density at the point x of the time t , Θ is the collision operator that determines the local distribution after the collision of particles.

Using LBM and equation (2) with respect to time, rewrite our equations for velocities as follows

$$f_i(\mathbf{x} + \mathbf{c}_i \Delta t, t + \Delta t) = f_i(\mathbf{x}, t) + \Theta_i(f), \quad (22)$$

where

$$\Theta_i(f) = -\frac{\Delta t}{\tau}(f_i - f_i^{eq}), \quad (23)$$

$$f_i^{eq} = w_i \left(1 + \frac{\mathbf{v} \cdot \mathbf{c}_i}{c_s^2} + \frac{(\mathbf{v} \cdot \mathbf{c}_i)^2}{2c_s^4} - \frac{\mathbf{v} \cdot \mathbf{v}}{2c_s^2} \right), \quad (24)$$

$$c_s^2 = \frac{1}{3} \cdot \left(\frac{\Delta x}{\Delta t} \right). \quad (25)$$

In equations (22)–(25), Δx and Δt are steps in space and time, f_i is the velocity distribution function (see figure 4), f_i^{eq} is the equilibrium distribution function, and τ is the dimensionless relaxation time

$$\tau = \frac{1}{2} + \frac{\alpha\mu}{c_s^2\Delta t}, \quad (26)$$

c_s is the speed of sound, which for the model D2Q9 has the form (25).

Discrete velocities c_i and the corresponding set of weight coefficients w_i form a set of velocities. There are different sets used in LBM.

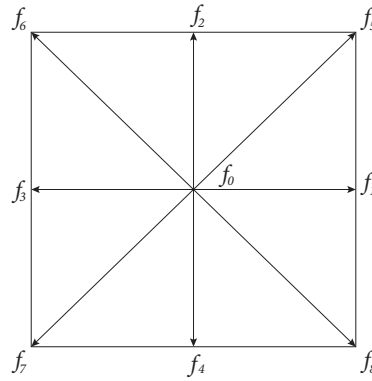


Figure 4. Model D2Q9 of discrete liquid flow rates.

Here 2 is the number of spatial dimensions (x and y), and 9 is the number of speeds

$$w_i = \begin{cases} 4/9, & i = 0, \\ 1/9, & i = 1, 2, 3, 4, \\ 1/36, & i = 5, 6, 7, 8, \end{cases}$$

$$\mathbf{c}_i = \begin{cases} (0, 0), & i = 0, \\ \left(\cos\left(\frac{\pi(i-1)}{2}\right), \sin\left(\frac{\pi(i-1)}{2}\right) \right), & i = 1, 2, 3, 4, \\ \sqrt{2} \left(\cos\left(\frac{\pi(i-5)}{2} + \frac{\pi}{4}\right), \sin\left(\frac{\pi(i-5)}{2} + \frac{\pi}{4}\right) \right), & i = 5, 6, 7, 8. \end{cases}$$

Equation (22) has two parts: collision and distribution. The particles move with the velocity \mathbf{c}_i to the neighboring node ($\mathbf{x} + \mathbf{c}_i\Delta t$) in time ($t + \Delta t$). In this case, the collision operator acts on them. Thus, the equation (22) can be split into two components

a) collision

$$f_i^*(\mathbf{x}, t) = f_i(\mathbf{x}, t) + \Theta_i(f);$$

b) distribution

$$f_i(\mathbf{x} + \mathbf{c}_i \Delta t, t + \Delta t) = f_i^*(\mathbf{x}, t).$$

After these two steps are completed, the distribution functions f_i are calculated for the current time step, and then the fluid velocity is found from

$$\mathbf{v} = \sum_{i=0}^8 f_i \mathbf{c}_i. \quad (27)$$

Similar transformations are carried out for displacements of the elastic soil frame described by the system of equations (5).

The product flux of chemical reactions can be described using the convection-diffusion equation [10]

$$\frac{\partial C_j}{\partial t} + \nabla \cdot (-\kappa_{c_j} \nabla C_j + \mathbf{v} C_j) = 0, \quad (28)$$

where C_j is the concentration of the products of chemical reactions j , κ_{c_j} is the dimensionless diffusion coefficient determined for each reaction product.

It is worth to note the absence of the term responsible for the chemical reaction, in view of the presence of the boundary conditions (8) and (9) at the “liquid-solid” interface.

The LB-analogue of the equation (28) will be as follows

$$g_i^j(\mathbf{x} + \mathbf{c}_i \Delta t, t + \Delta t) = g_i^j(\mathbf{x}, t) + \Theta_i^j(g), \quad (29)$$

where

$$\Theta_i^j(g) = -\frac{\Delta t}{\tau_g} (g_i^j - g_i^{eq,j}), \quad (30)$$

$$g_i^{eq,j} = w_i C^j \left(1 + \frac{\mathbf{v} \cdot \mathbf{c}_i}{c_s^2} \right). \quad (31)$$

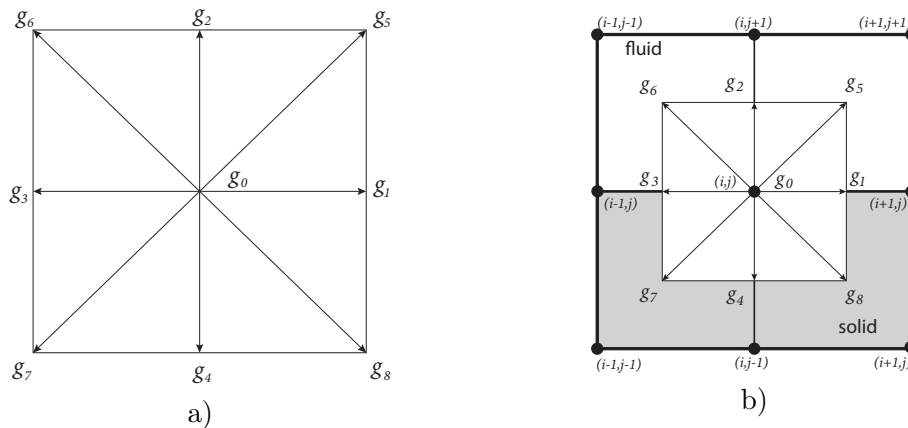


Figure 5. a) model D2Q9 of discrete mass transfer rates; b) concentration distribution at the liquid-solid interface.

Solving equations (29)–(31), find the concentration in equation (28)

$$C^j = \sum_{i=0}^4 g_i^j. \quad (32)$$

Since the time scale of fluid flow is much smaller than other processes, the velocity reaches steady state during the selected time step. The equilibrium distribution functions are calculated using the equation (31), then the collision step (see figure 5a) is performed according to the following equation

$$g_i^{j*}(\mathbf{x}, t) = g_i^j(\mathbf{x}, t) + \Theta_i^j(g). \quad (33)$$

The concentration distribution functions near the “liquid-solid” interface (see figure 5b) will have the following form

$$\sum_i g_i \mathbf{e}_i = \kappa_c \frac{\partial C^j}{\partial n} + \beta C^j. \quad (34)$$

Since the time scale of fluid flow is much smaller than other processes, the velocity reaches steady state during the selected time step. The equilibrium distribution functions are calculated using the equation (31), then the collision step is performed according to the following equation

$$g_i^{j*}(\mathbf{x}, t) = g_i^j(\mathbf{x}, t) + \Theta_i^j(g). \quad (35)$$

The geometry of elastic solid frame is updated using the rules detailed in [11]. Before performing the propagation stage, to apply the rock dissolution effect, first update the distribution function and then calculate the propagation stage

$$g_i^j(\mathbf{x} + \mathbf{C}_i \Delta t, t + \Delta t) = g_i^{j*}(\mathbf{x}, t). \quad (36)$$

After that, solving (32) obtain the concentrations of the products of chemical reactions and proceed to the next time step.

As stated earlier, the multiple relaxation in time (MRT) scheme [12] is used to improve the stability of calculations. This scheme uses the transformation matrix M . Thus, the collision operator will be

$$\Theta_i(f) = - \sum_k (M^{-1} S M)_{ik} (f_k(\mathbf{x}, t) - f_k^{eq}(\mathbf{x}, t)), \quad (37)$$

where $S = \text{diag}(0, s_e, s_\epsilon, 0, s_q, 0, s_q, s_v, s_v)$ is a diagonal matrix.

The parameters s_v and the relaxation time τ are related as

$$s_v = \frac{1}{\tau}.$$

To improve accuracy, it is extremely important to choose the correct relaxation parameter values. Thus the establishment of so-called viscous relationship between s_q and s_v [13] is used to reduce the nonphysical behavior of fluid near the free boundary in the course of numerical solution

$$s_q = \frac{4(2 - s_v)}{4 + 7s_v}.$$

For s_e and s_ϵ

$$s_e = s_\epsilon = s_v.$$

3.1. Immersed boundary method (IBM)

The immersed boundary method is used to track the free boundary behavior. The main idea of the IB method is that the flow field is influenced by the force distribution created by the free boundary of the solid body. IBM uses independent meshes for fluid and solid sampling. The fluid is discretized by a set of Eulerian points, which are in fact fixed regular Cartesian lattice points, and the body boundary is discretized by a set of Lagrangian markers.

In LBM, the fluid velocity \mathbf{v} is calculated from the intermediate velocity \mathbf{v}^* and the correction $\delta\mathbf{v}$. With the IB method, the velocity corrections at the Lagrangian points are distributed over the Euler points. If the Lagrangian points are on the free boundary $\mathbf{X}_b(s_l, t)$, $l = 1, 2, \dots, m$, where m is the number of points, then the velocity corrections $\delta\mathbf{v}$ for the Euler points will be

$$\delta\mathbf{v}(\mathbf{x}, t) = \int_{\Gamma} \delta\mathbf{v}_b(\mathbf{X}_b, t) \delta(\mathbf{x} - \mathbf{X}_b(s, t)) ds, \quad (38)$$

$$\delta(r) = \begin{cases} \frac{1}{4}(1 + \cos(\frac{\pi|r|}{2})) & |r| \leq 2 \\ 0 & |r| > 2 \end{cases} \quad (39)$$

where r is the distance between any points of the considered region $\mathbf{x} \in \Omega$ and $\mathbf{X}_b(s, t) \in \Gamma$. Using equations (38) and (39) for two spatial variables, we get

$$\delta\mathbf{v}(\mathbf{x}_{ij}, t) = \sum_l \delta\mathbf{v}_b^l(\mathbf{X}_b^l, t) \delta_{ij}(\mathbf{x}_{ij} - \mathbf{X}_b^l) \Delta s_l, \quad l = 1, 2, \dots, m, \quad (40)$$

Δs_l is the arc length of the boundary element. Now the velocity at the Euler points can be adjusted as follows

$$\mathbf{v}(\mathbf{x}_{ij}, t) = \mathbf{v}^*(\mathbf{x}_{ij}, t) + \delta\mathbf{v}(\mathbf{x}_{ij}, t). \quad (41)$$

The last equation is the key point that unites the LB and IB methods.

According to the boundary condition (7), the velocities of the liquid at the boundary points must be equal to the velocities of the solid boundary

$$\mathbf{v}_b^l(\mathbf{X}_b^l, t) = \sum_{i,j} \mathbf{v}(\mathbf{x}_{ij}, t) D_{ij}(\mathbf{x}_{ij} - \mathbf{X}_b^l) \Delta x \Delta y, \quad (42)$$

where \mathbf{v}_b^l are the local velocities of the free boundary.

When simulating the interaction of a fluid and an elastic body, it is necessary to know the velocities of all points of the free boundary. For this, we used the finite element method (FEM). The main condition on the “fluid-solid” interface is the following condition

$$(\kappa_\mu \sigma(x, \mathbf{v}^\varepsilon) - p^\varepsilon \mathbb{I}) \cdot \mathbf{n} = (\kappa_\lambda \sigma(x, \mathbf{w}^\varepsilon) - p^\varepsilon \mathbb{I}) \cdot \mathbf{n}. \quad (43)$$

The use of LBM and FEM for fluid-structure interaction was carried out in a checkerboard pattern. In other words, the LBM was applied to the liquid component using the velocity obtained at the interface using FEM. This cycle continued until the condition (43) followed. The return path was applied to the points of the free boundary. When the distribution of particles reaches the boundary point of the lattice, then they are scattered back to the node where they came from.

To preserve the continuity of the velocities at the “fluid-solid” interface, the local distribution of particles f_i was additionally modified [14]. If v_x^- and v_y^- be the components of the difference between velocities of an elastic body and a fluid along the axes x and y on the free boundary, then

$$\begin{aligned} f_2 &\leftarrow f_2 + \frac{\Delta v_x^s}{3}, \\ f_3 &\leftarrow f_3 + \frac{\Delta v_y^s}{3}, \\ f_4 &\leftarrow f_4 - \frac{\Delta v_x^s}{3}, \end{aligned}$$

$$f_5 \leftarrow f_5 - \frac{\Delta v_y^s}{3}$$

$$f_6 \leftarrow f_6 + \frac{\Delta v_x^s}{12} + \frac{\Delta v_y^s}{12}, \quad f_7 \leftarrow f_7 - \frac{\Delta v_x^s}{12} + \frac{\Delta v_y^s}{12}$$

$$f_8 \leftarrow f_8 - \frac{\Delta v_x^s}{12} - \frac{\Delta v_y^s}{12}, \quad f_9 \leftarrow f_9 + \frac{\Delta v_x^s}{12} - \frac{\Delta v_y^s}{12}$$

This is followed by a finite element analysis.

3.2. Numerical results

By solving the system of equations (1)–(19) distribution of chemical reaction products and reagent concentration at different moments of dimensionless time were obtained.

Thus, in figure 6 you can see the change in the concentration of chemical reaction products at different $t=[4.2 \cdot 10^3; 1.6 \cdot 10^4; 2.6 \cdot 10^4; 1.1 \cdot 10^5]$.

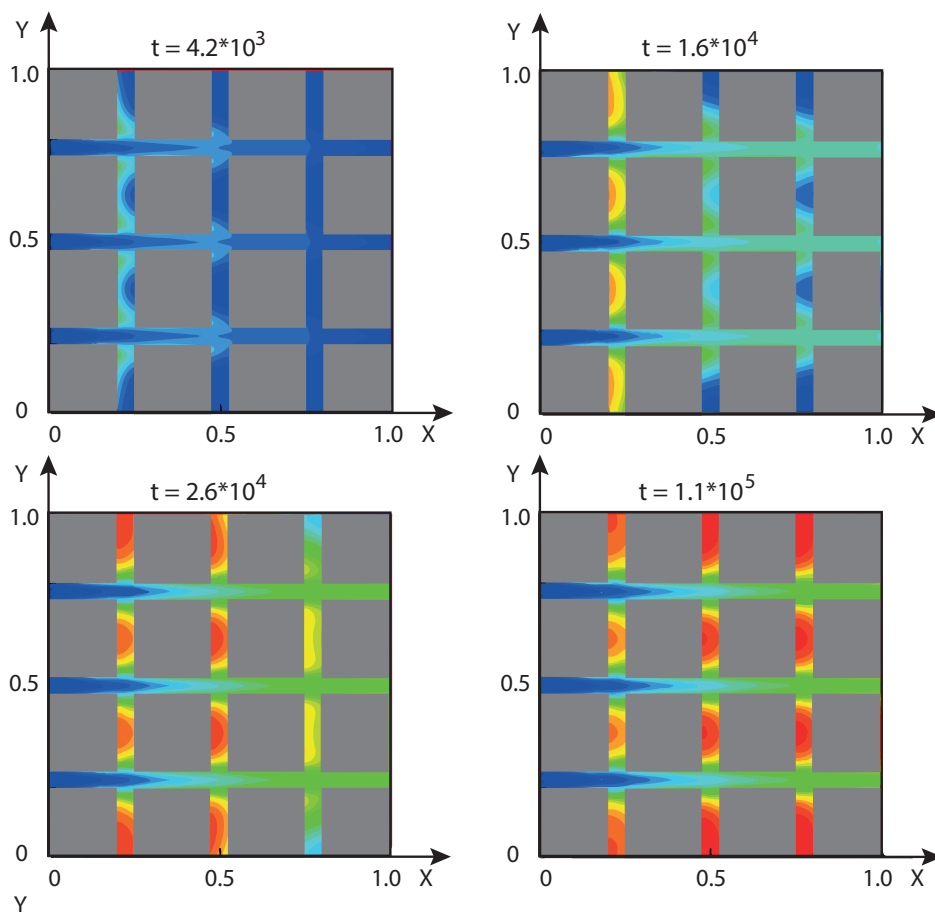


Figure 6. Chemical reaction products at different dimensionless time moments.

Similar results are observed when simulating the propagation of an acid solution. Figure 7 shows that the elastic soil frame dissolves completely over time $t=[4.2 \cdot 10^3; 1.6 \cdot 10^4; 2.6 \cdot 10^4; 1.1 \cdot 10^5]$.

Let us note the importance of coefficient β in the condition on the free boundary. It affects the dissolution rate of elastic solid frame. Figure 8 shows the concentration field of the reagent with $\beta = [1; 10]$ at fixed time moment $t=2.7 \cdot 10^5$.

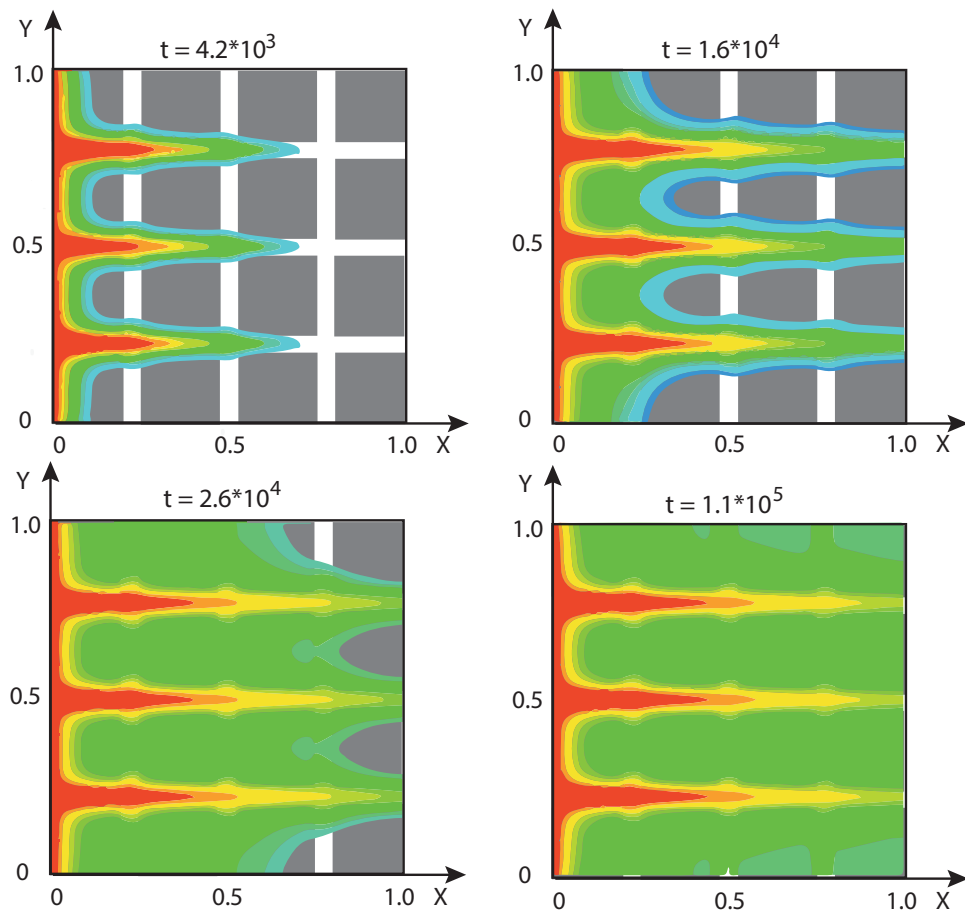


Figure 7. Reagent concentration at different dimensionless time moments.

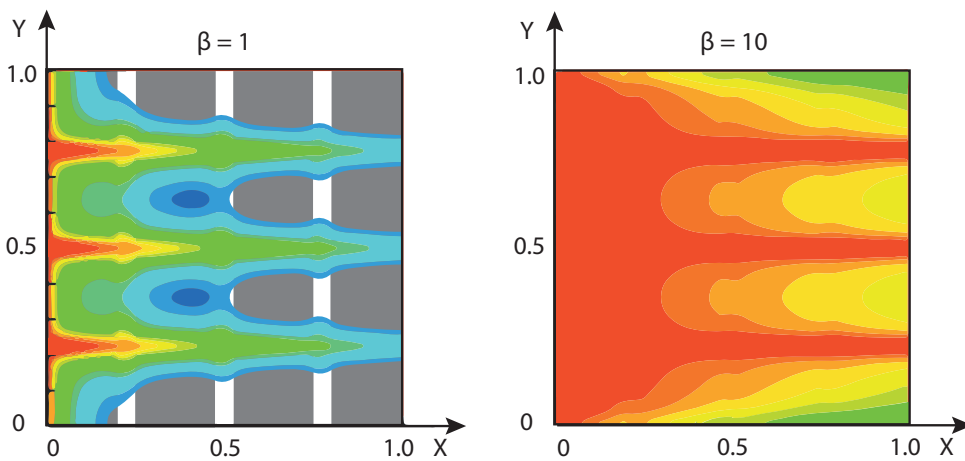


Figure 8. Reagent concentration for different values of β at fixed dimensionless time moment.

Finally, figure 9 shows the position of the free boundary at fixed time moment $t=1 \times 10^6$. The gray borders denote the geometry of elastic soil frame before acid exposure.

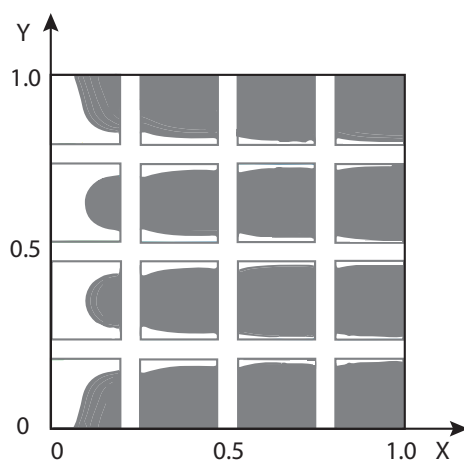


Figure 9. The free boundary position at fixed time moment.

Acknowledgments

This research was supported by the Russian Science Foundation (project No 19-71-00105).

Conclusion

In this study, a correct mathematical model for cleaning the bottomhole zone of oil wells was derived based on the fundamental laws of continuum mechanics and theoretical chemistry, which accurately describe the physical processes under consideration at the microscopic level (on the scale of pores and cracks). The problem of acid treatment of a non-periodic elastic solid frame with double porosity was considered. Numerical experiments of the problem are carried out. The influence of acid concentration in the injection well and coefficients in the condition on the common boundary “liquid-elastic solid body” is investigated. On each temporarily layer, the border was adjusted twice. First, as a result of fluid action on an elastic body, then as a result of acid dissolution. As a result, an increase in the products of the chemical reaction can be noted over time at a given value of the concentration of the reagent at the inlet boundary. Also revealed the influence of the coefficient β in the condition on the free boundary. With its increase, the dissolution process proceeds faster.

References

- [1] Kalia N and Balakotaiah V 2009 *Chem. Eng. Sci.* **64** 376
- [2] Cohen C *et al.* 2008 *Chem. Eng. Sci.* **63** 3088
- [3] Panga M, Ziauddin M and Balakotaiah V 2005 *A.I.Ch.E. Journal* **51** 3231
- [4] Meirmanov A, Galtsev O and Zimin R 2017 *Free boundaries in rock mechanics* (Berlin: Walter de Gruyter)
- [5] Meirmanov A 2010 *Math. Models Methods Appl. Sci.* **20** 635
- [6] Ovsyannikov L 1977 *Introduction to Continuum Mechanics* (Novosibirsk: Novosibirsk State University)
- [7] Kenneth W *et al.* 2014 *Chemistry* 10th ed (Brooks: Belmont)
- [8] Meirmanov A 2010 *Math. Models Methods Appl. Sci.* **20** 635
- [9] Kruger T *et al.* 2017 *The Lattice Boltzmann Method* (Berlin: Springer)
- [10] Steefel C 2015 *Comput. Geosci.* **19** 445
- [11] Patel R *et al.* 2014 *Phys. Chem. Earth* **70** 127
- [12] Humiere D 1992 *Prog. Astronaut. Aeronaut.* **159** 450
- [13] Lu J *et al.* 2012 *Phys. Rev. E* **85** 016711
- [14] Kwon Y 2006 *Eng. Comput.* **23** 860